Manipulation and filtration of low index particles with holographic Laguerre-Gaussian optical trap arrays

P. A. Prentice[1], M. P. MacDonald[2], T. G. Frank[3], A. Cuschieri[3], G. C. Spalding[4], W. Sibbett[2], P. A. Campbell[1,2] and K. Dholakia[2]

[1.] *Department of Surgery and Molecular Oncology, Ninewells Hospital, University of Dundee, Dundee DD1 9SY. Scotland.*
[2.] *School of Physics and Astronomy, St Andrews University, North Haugh, St Andrews, Fife KY16 9SS. Scotland.*
[3.] *Institute for Medical Science and Technology, Ninewells Hospital, University of Dundee, Dundee DD1 9SY. Scotland*
[4.] *Department of Physics, Illinois Wesleyan University, PO Box 2900, Bloomington 61702-2900, IL. USA.*
p.a.campbell@dundee.ac.uk

Abstract: Multiple low index particles (micrometer-sized ultrasound contrast agent), have been optically trapped using a 4 x 4 Laguerre-Gaussian trap array. The trapping efficiency of the Laguerre-Gaussian arrangement was measured using a Stokes' flow approach whereby the critical relative fluid velocity required to remove particles from the optical trap was measured. The dependence of trapping efficiency on beam power was also explored and the optimum beam parameters were identified. Finally, the utility of the array as a selective filter was demonstrated by tweezing multiple low-index particles from a population exhibiting an inherent distribution in size. This procedure represents a unique remote non-contact process that may have significant applicability throughout the fields of biophysics and biotechnology.

OCIS codes: (090.2890) Holographic optical elements; (140.7010) Trapping

References

1. A. Ashkin J.M. Dziedzic, J.E. Bjorkholm & S. Chu, "Observation of a single beam gradient force optical trap for dielectric particles," Opt. Lett.**11**, 288 (1986)
2. S. Sato & H. Inaba, "Achievement of laser fusion of biological cells using UV pulsed laser beams," Appl. Phys. B **54**, 531 (1992)
3. H. Liang, W.H. Wright, C.L. Rieder, E.D. Salmon, G. Proteta, J. Andrews, Y.G. Liu, G.J. Sonek, M. Berns, "Micromanipulation of chromosomes in PtK2 cells using laser microsurgery in combination with laser induced optical forces," Experimental Cell Res. **204**, 110 (1993)
4. M.P. MacDonald, L. Paterson, K. Volke-Sepulveda, J. Arlt, W. Sibbett, K. Dholakia, "Creation and manipulation of three-dimensional optically trapped structures," Science **296**, 1101 (2002)
5. V.Garces-Chavez, D.McGloin, H.Melville, W.Sibbett, K.Dholakia, "Simultaneous micromanipulation in multiple planes using a self reconstructing light beam," Nature **419**, 145 (2002)
6. K.T. Gahagan, G.A. Swartzlander, "Simultaneous trapping of low index and high index microparticles observed with an optical vortex trap," J. Opt. Soc. Am. B **16,** 533(1999)
7. K.T. Gahagan, G.A. Swartzlander, "Trapping of low index particles in an optical vortex," J. Opt. Soc. Am. B **15,** 524 (1998)
8. M.P. MacDonald, L. Paterson, W. Sibbett, K. Dholakia & A. Riches, "Trapping and manipulation of low index particles in a 2D interferometric trap," Opt. Lett. **26,** 863 (2001)
9. P.J. Rodrigo, R.E. Eriksen, V.R. Daria & J. Gluckstad, "Shack Hartman multiple beam optical tweezers," Opt. Express **11,** 208 (2003), http://www.opticsexpress.org/abstract.cfm?URI=OPEX-11-3-208.

#3693 - $15.00 US Received 6 January 2004; revised 5 February 2004; accepted 8 February 2004

10. E.R. Dufresne, G.C. Spalding, M.T. Dearing, S.A. Sheets & D. Grier, "Computer generated holographic optical tweezer arrays," Rev. Sci. Instruments **72**, 1810 (2001)
11. J. Voros, "The density and refractive index of absorbing protein layers," (to be published in Biophysical Journal (2004))
12. N.B. Simpson, L. Allen, M.J. Padgett "Optical tweezers with increased axial trapping efficiency," J. Mod. Opt. **45**, 1943 (1998)
13. A.T. O'Neill, M.J. Padgett, "Axial and lateral trapping efficiency of Laguerre Gaussian modes in inverted optical tweezers," Opt. Commun. **193**, 45 (2001)
14. W.H. Wright, G.J. Sonek, M.W. Berns, "Parametric Study of the forces on microspheres held by optical tweezers," Appl. Opt. **33**, 1736 (1994)
15. K.T. Gahagan, G.A. Swartzlander. "Optical vortex trapping of particles," Opt. Lett. **21**, 827 (1996)
16. R.C. Gauthier, "Laser trapping properties of dual component spheres," Appl. Opt. **41**, 7135 (2002)

1. Introduction

Optical tweezing typically involves the use of tightly focussed laser beams to trap and subsequently manipulate micron and sub-micron sized particles. Pioneered by Ashkin [1], optical trapping has since undergone rapid development and has attracted particular attention from those working at the life-sciences interface. This is because optical traps are operated remotely and therefore have an intrinsic non-invasive/non-contact nature which allows manipulation of samples with reduced risk of contamination or physical damage. One exemplar application of optical trapping within the field of biology has involved the development of all-optical cell fusion [2]. Further innovation has seen the use of laser light as an 'optical scalpel' for the dissection of chromosomes: the divided sections being subsequently manipulated via a trapping laser [3].

More recently, advances in photonics have injected new impetus to the field. In particular, the advent of spatial light modulators (SLMs) and computer generated holography (CGH) have facilitated optical trapping with added degrees of freedom. Such approaches have allowed controlled rotation of multiply trapped particles using novel interference patterns [4], as well as in zeroth and higher order non-diffracting Bessel beams [5].

For the present work, we employed CGH to generate special beam arrays for the trapping and manipulation of clinically relevant low index particles (ultrasound contrast agent (UCA)). Previous work on low index particle trapping has been limited to either single hollow particles [6], or else the trapping of high-index/low-index particle pairs in either vortex beams [7], or interferometric traps [8]. Further, whilst the utilisation of trapping arrays has become more prevalent since the introduction of SLMs [9], there has been no demonstration, until now, of tweezing multiple low index particles within a spatially extended planar trapping array. Here we use a 4 x 4 array of Laguerre-Gaussian (LG) traps to filter low index particles from a population. Moreover, we have characterised the trapping efficiencies of such arrays in a dynamic environment (relative fluid motion), and also as a function of the beam parameters. This work underscores the usefulness of LG trapping arrays within the arena of micro-fluidics, and related biophysical contexts.

2. Apparatus, materials and methods

2.1 Experimental set-up

The tweezers system used for this work was based on a Zeiss Plan Neofluar objective lens exhibiting x63 magnification and a numerical aperture, NA = 0.9. A schematic of the experimental set-up is illustrated in Fig. 1 below. The trapping beam originated as the TEM_{00} (l=0) mode from a Nd:YVO_4 solid state laser operating at 1064 nm and is collimated using lens L1. In order to generate multiple trapping sites with a specific trap intensity profile, two holograms are utilised within the optical path. The first, a computer generated hologram (designated H1 in Fig.1.), endows the collimated laser beam with the desired intensity profile by encoding for a Laguerre-Gaussian mode (with l=3). The character of the resultant LG beam is often described as an 'optical vortex': the light distribution at the focal place has zero

#3693 - $15.00 US Received 6 January 2004; revised 5 February 2004; accepted 8 February 2004

intensity on the optical axis, and this is surrounded by a high intensity annulus. As the LG beam traverses the remainder of the optical path lenses L2 and L3 resize the beam to fill the etch pattern of a second hologram (H2 in Fig. 1). H2 acts as a diffractive optic element (DOE) that splits the single incident LG beam into a defined distribution. Lenses L4 and L5 are 100mm plano-convex lenses which produce a point conjugate to the back aperture of the objective lens, halfway between these lenses. This is useful for aligning the beam axis to the optical axis of the system, and allows blocking of any central undiffracted orders from the DOE (H2). The DOE was itself produced in-house following the prescription of Dufresne *et al* [10]. The specific arrangement employed for the experiments is termed a 'hexa-deca tweezer' as it gives rise to a 4 x 4 array of optical traps, as illustrated in Fig. 2 below. The design was generated by a numerical iteration technique and fabricated via photolithography and reactive ion etching onto a fused silica substrate. Complete details of the holographic elements are available elsewhere [10].

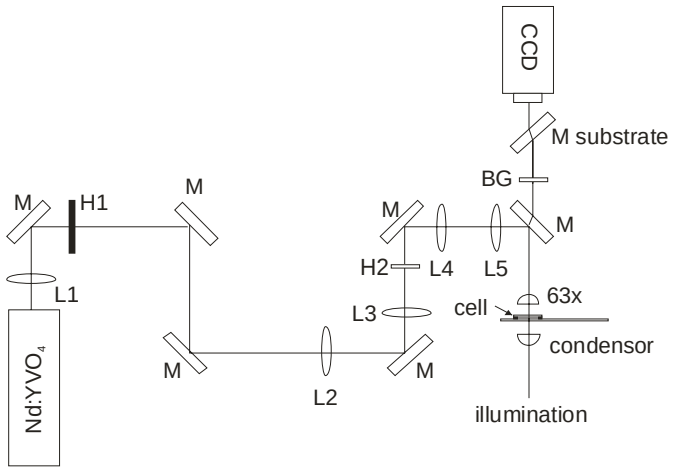

Fig. 1. Schematic of tweezing set-up. L – lens, M – Mirror, H1 – LG hologram, BG – IR filter, H2 – 4x4 hologram.

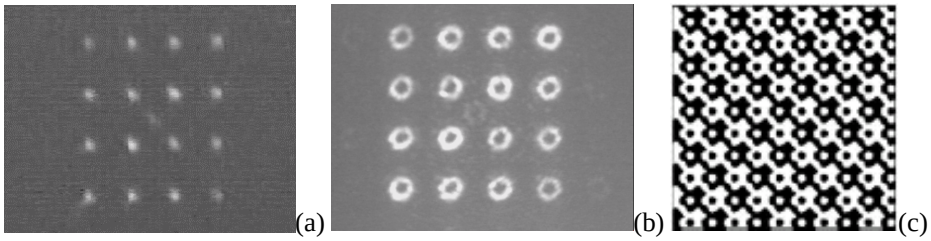

Fig. 2. (a) The intensity distribution at the focal plane of the objective on illuminating the hexadeca DOE with a standard Gaussian beam. (b) The intensity distribution on illuminating the DOE with an LG *l*=3 beam (i.e. after insertion of H1 into the optical path. Each annulus has the potential to trap a low index particle of suitable diameter. (c) A binary level version of the pattern used to produce the 4 x 4 spot intensity distribution of (a) and (b). The black regions shift the phase by π radians.

2.2 Materials

The UCA employed was commercially available Optison® microbubbles, which consist of an albumin shell encapsulating octofluropropane gas cores. The particles have diameters within the range 2-7μm, according to the manufacturer's specifications. The refractive indices of the

#3693 - $15.00 US Received 6 January 2004; revised 5 February 2004; accepted 8 February 2004

component materials are assumed to be unity and 1.42 [11] for the gas core and shell respectively.

A solution comprising 20μl of UCA, mixed thoroughly with deionised water, was placed in a sample chamber consisting of a microscope slide, a 70μm spacer and a coverslip. For preliminary single micro-bubble trapping, a dilute sample (with a concentration of 10^5 UCA particles/ml) would be prepared, which typically led to between 10 – 20 particles being visible within the field of view. Such a concentration is low enough to avoid any hydrodynamic coupling between the particles, and thus assists with the implementation of a simple model for their analysis, as outlined below. The chamber was then mounted on a programmable actuator-controlled (Newport CMA-25PP) x-y-z translation stage so that trapped UCA could be scanned linearly and with controllable speeds, through the solution.

2.3 Analytical approach

As the experiments operated in the ray-optic regime, where the diameter of the particle is larger than the wavelength of the trapping laser light, therefore the dominant physical process involves the refraction of light at the solution-particle interface. In the case of standard trapping, where a Gaussian beam is used to trap a particle of higher refractive index than that of the surrounding medium, differential refraction occurs across the intensity gradient of the beam which yields a net force on the particle that is directed towards the focus of the beam and establishes a state of stable equilibrium.

Conversely, a particle of lower refractive index than the medium (as is the case with UCA in deionised water) will experience a gradient force that repels it from the regions of greatest intensity. Therefore, if an optical trap is to be used to contain particles of lower refractive index, it should contain a region of lower intensity, surrounded by a containing region of higher intensity potential barrier.

Further, not all the incident light is refracted when using Gaussian trapping beams: scattering from the particle surface results in a secondary force in the direction of beam propagation, which acts to reduce the overall axial trapping force, as we discuss later. Therefore, in order to address the low index nature of our target particles, and also to combat the effects of scattering, the rationale for employing LG beams as the basis for trapping is obvious as the intrinsic toroidal morphology of this mode minimizes the effects of scattering without compromising the trapping force. This ensures that the trapped low index particles are located within the dark region that is surrounded by the high intensity annulus.

As our target particles for trapping exhibit diameters in the range 2-7μm, the spatial extent of the LG trap annulus must be tailored to comparable dimensions. The equation relating an annulus' radius of maximum intensity, r_{max} is related to the azimuthal *l*-index of the mode thus:

$$r_{\max} = \omega\sqrt{\frac{l}{2}} \tag{1}$$

where ω is the radius at which the Gaussian term in the LG polynomial falls to 1/e of its on-axis value. We found that an $l = 3$ mode generated an annulus of appropriate size (circa 6μm).

The force with which an optical trap contains a particle, F_{trap}, may be described in terms of a dimensionless parameter known as the trapping efficiency, Q, thus:

$$F_{trap} = Q\frac{n_o P}{c} \tag{2}$$

where n_o is the refractive index of the containing medium, P is the incident power of the laser, c is the speed of light. Further, the trapping efficiency may be resolved into both an axial efficiency, Q_{axial}, (in the direction of beam propagation), and also a lateral efficiency, $Q_{lateral}$, (in the direction perpendicular to beam propagation).

In order to experimentally determine the efficiency of the traps thus generated, we introduced relative motion between the trapped particle and the solution in order to generate a

#3693 - $15.00 US Received 6 January 2004; revised 5 February 2004; accepted 8 February 2004

Stokes' drag force, after the fashion of Simpson *et al* [12] and also O'Neill and Padgett [13]. The procedure involved the gradual increment of the scanning trap velocity (which is directed orthogonally to the laser beam axis) to the point upon which the particle was removed from the trap: this is termed the critical velocity, v_c. Whilst the hydrodynamics of the situation is slightly complicated by the actual thickness of the water layer involved [14], we merely applied Stokes' law directly to the situation in order to achieve an approximation to the drag force, F_{drag}, exerted on the trapped particle:

$$F_{\text{drag}} = 3\pi\eta v d \tag{3}$$

Here, the viscosity of the liquid is represented, η, the flow velocity by v, and the diameter of the particle as d. Therefore, equating the expressions for F_{trap} and F_{drag} (Eqs. (2) and (3)) at the critical point allows a simple expression for $Q_{lateral}$ in terms of v_c and P thus:

$$Q_{lateral} = \frac{c}{n_o}\frac{3\pi\eta v_c d}{P} \tag{4}$$

The axial trap efficiency may also be investigated using the Stokes' flow method. However, the depth of the chamber employed here limits the range of velocities that may be used. In order to measure the axial efficiency of the trap, we determined the minimum laser power required in order to trap a particle against gravity and thermal motion, thus:

$$F_{\text{min}} = \frac{\pi}{6}(\rho_p - \rho_m)d^3 g + \frac{2kT}{d} \tag{5}$$

where ρ_{p} and ρ_{m} are the densities of the trapped particle and medium respectively, and g, k and T represent acceleration due to gravity, Boltzmann's constant, and temperature (in Kelvin) respectively. Equating (2) and (5) gives us an expression for Q_{axial} in terms of P_{min}, the power below which the particle becomes free and floats back to the top of the chamber under its natural buoyancy. Given this escape mechanism it is only possible to determine Q_{axial} for trapping away from the coverslip.

3. Results

3.1 Individual UCA Trapping

UCA particles were trapped both against, and away from, the upper glass surface of the sample chamber. The former case was achieved simply by allowing the hollow UCA to rise up through the chamber under the action of buoyancy forces. The specific procedure for trapping individual UCA particles was to: (i) block the beam before the objective lens; (ii) align its position over an UCA particle of suitable diameter as dictated by the size of the beam core; (iii) unblock the beam. Planar (x-y) manipulation of the particle could be achieved through translation of the sample stage or by controlling the steering mirror at the objective back aperture. Manipulation in the z-direction was demonstrated by raising the stage upwards towards the tweezing objective. The trapped particle remained in a stationary position as the free UCA particles rose up with the coverslip of the chamber. If the sample stage was subsequently lowered, away from the tweezing objective, the trapped particle would remain in the focal region as the free particles descended below the coverslip. These observations suggest that each UCA particle is trapped below the focal point of the beam, within the vortex core.

It was found that particles with estimated diameters in the range 4 to 5 μm were trapped most readily with the optical set-up described. These were then subjected to critical velocity measurements. The graphs in Figs. 3 and 4 below display the results obtained of critical velocity versus the incident laser power. Each data point represents the average of at least 5

#3693 - $15.00 US Received 6 January 2004; revised 5 February 2004; accepted 8 February 2004

measurements that were repeated with the same particle. Equivalent results for the trapping of high refractive index polymer spheres in an LG *l*=1 beam are presented for comparison.

For comparative purposes, we also analysed the performance of the LG beam in trapping an alternative low index particle in the form of micrometer-sized hollow glass spheres. As has been reported previously, hollow particles exhibiting thick (relative to the size of the gas core) shells, do not always behave as low index particles. Rather, they may be attracted to high intensity regions in the manner of solid glass spheres (i.e., high index particles) [15]. In our experiments, smaller hollow glass spheres would typically be perceived as high index particles by the beam, and therefore be attracted to high intensity regions. On the other hand, larger hollow glass spheres would be perceived as low index particles and repelled from the high intensity regions. A noteworthy observation made during the present work was that all UCA particles, irrespective of size, behaved as low index particles. These micro-bubbles were always repelled from the high intensity annulus, either into the vortex trap or away from the beam altogether. These observations can be reconciled within the enhanced ray-optic model developed by Gauthier [16], where the subtleties of photon momentum change at specific optical interfaces within the dual component (i.e. shelled microbubble) system are considered, in terms of their contribution to the trapping force, as a function of the beam, medium, and microbubble parameters.

Particles were liberated from the optical trap when the Stokes' force just exceeded the trapping force. Here, the escape route of individual UCA particles was downwards along the boundary between the low intensity cone, formed by the core, and the high intensity envelope. It should be noted that particles were subjected to prolonged drag forces in order to obtain these critical velocity measurements in order to allow the full fluid dynamic environment to develop and equilibrate. Over much shorter scan durations, the particles would remain trapped for much larger relative flow velocities than those recorded here. This observation may be significant for optimising throughput in specific micro-fluidic devices.

Analysis allows an explanation for the saturation feature dominant in Fig. 4. When the power of the incident beam was increased with a UCA particle resident within the trap, then the particle was seen to move slightly downwards, under the action of the scattering force. Thus, the particle would be, in effect, pushed towards its escape route, even before relative flow conditions were initiated. Therefore, any strengthening of the lateral trapping force achieved by increasing the laser intensity, was effectively compromised as the particle was pushed down and out of the focal plane. This effect is mirrored in the deviation from linearity in the graph of Fig. 4 for any pumping current over circa 0.8A. In calculating the trapping efficiency Q values of Table 1 below, only the low pumping current measurements have been used.

Table 1. Average values of Q-lateral and Q-axial for CA micro-bubbles optically trapped in a Laguerre-Gaussian *l*=3 beam, as calculated using equations (4) and (5).

	$Q_{lateral}$	Q_{axial}
Against Surface	0.0137±0.0096	-
Away from Surface	0.0215±0.0092	0.00815±0.00122

#3693 - $15.00 US Received 6 January 2004; revised 5 February 2004; accepted 8 February 2004

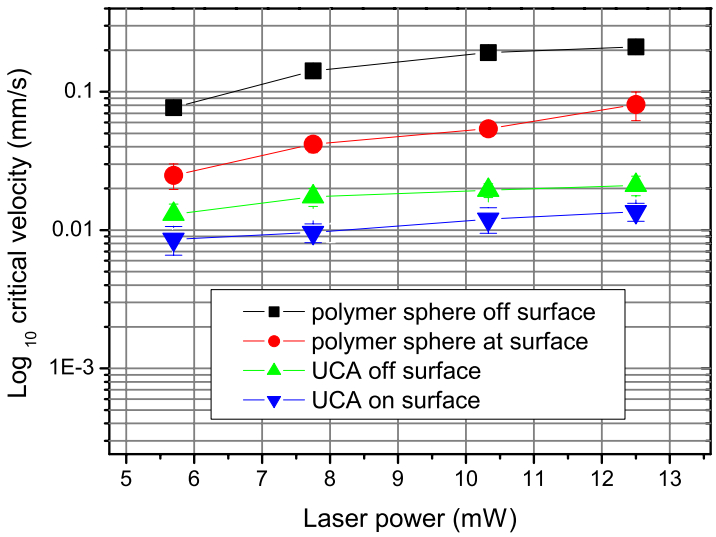

Fig. 3. Logarithm of the critical velocity required to displace both high and low index particles from the optical trap versus the laser power. The effect of location is also apparent: in both instances, there is a marked increase in critical velocity when the particles are trapped away from a solid surface.

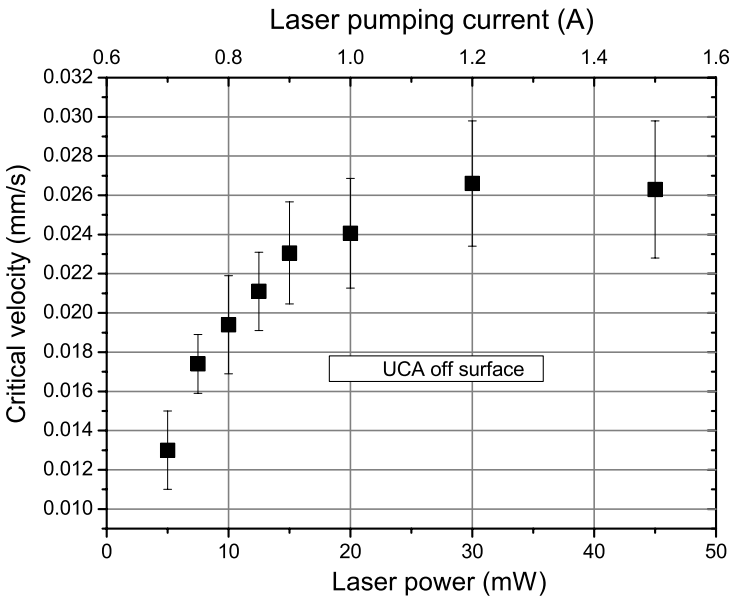

Fig. 4. Graph of critical velocity required to laterally displace the CA particle from the optical trap, versus the laser power (and equivalent pumping current). There is no enhancement in trapping efficiency beyond laser powers of around 30mW as the effects of scattering push the particles further below the trap plane.

#3693 - $15.00 US Received 6 January 2004; revised 5 February 2004; accepted 8 February 2004

3.2 Multiple UCA Trapping

For the case of multiple trapping the sample solution was prepared with a typical concentration of 10^7 particles/ml. This ensured a reasonable probability for trapping multiple particles when the beam is unblocked. Figure 5 below is a representative observation obtained as the sample chamber was raised towards the tweezing objective. Eight UCA particles, with diameters within the specific range 4-5 microns, have been trapped and are held as the rest of the micro-bubbles rise with the sample. Note that the traps on the bottom-left to top-right diagonal are strongest and have all been filled. Also apparent are the empty trap positions in the plane containing the free particles. These areas have been cleared as free low index particles are repelled from regions of high intensity. This observation indicates a possible application of such trap arrays as selective [spatial] particle filters.

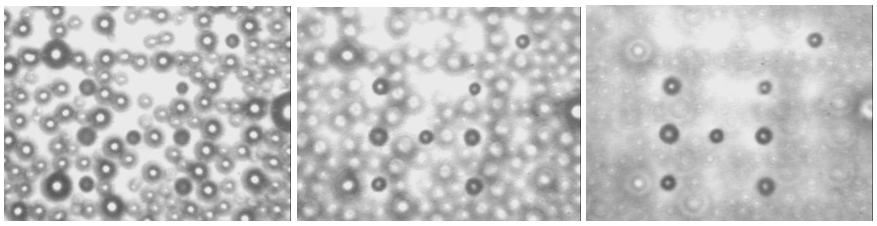

Fig. 5. Photomicrographs demonstrating optical manipulation of 8 micro-bubbles simultaneously out of the plane of the top of the sample. In the left-most image, the trap array is established within a population of the contrast agent micro-bubbles, trapping 8 particles in the process. In the subsequent images, the array plane is physically moved in the z-direction so that trapped particles are selectively and simultaneously removed away from the rest of the population.

4. Conclusion

We have demonstrated that multiple low index particles can be trapped and manipulated in 3D via holographic LG arrays. An immediate application is the selective filtration of specific particle sizes from a population exhibiting a larger distribution in size. The specific low-index particle that we have trapped (UCA) has continually widening applicability within the biophysical field. We anticipate that the facility to trap this type of particle in optical trap arrays may have potential application in various theatres of operation, including that of drug delivery.

Acknowledgments

We acknowledge financial support from the UK EPSRC (Grants GR/R88502/01 and GR/88496/01) and the SHEFC, through the award of an SRDG grant. A private communication with Janos Voros (ETH Zurich) regarding the refractive index of albumin is also gratefully acknowledged.